

# SURVEY AND ANALYSIS OF LINE-FREQUENCY INTERFERENCE IN THE CEBAF ACCELERATOR \*

M. G. Tiefenback and Rui Li, Continuous Electron Beam Accelerator Facility, 12000 Jefferson Avenue,  
Newport News, VA 23606 USA

RECEIVED

JUL 25 1996

OSTI

Feedthrough of interference from the AC power line into accelerator components is a problem which in pulsed accelerators can be reduced by operation synchronous with the AC line. This means of avoiding line-frequency effects is ineffective for continuous wave machines such as the CEBAF accelerator. We have measured line-frequency perturbations at CEBAF both in beam position and energy by using the beam position monitor system as a multiple-channel sampling oscilloscope. Comparing these data against the measured static optics (taken synchronously with the AC line) we have been able to identify point sources of interference, and resolve line-synchronous variations in the beam energy at a level near 0.001%.

## I. INTRODUCTION

The design specifications for the CEBAF electron beam (4 GeV, 200 microampere, continuous wave) include a spot size and stability on target of approximately 100 microns and a geometric beam emittance of  $2 \cdot 10^{-9}$  meter radian at 1 GeV. Time averages of these parameters are important and can be significantly degraded by line-frequency interference. In addition, there are several septa in the accelerator which have beam clearances of only a few millimeter; beam position perturbations at these locations could result in beam loss and interruptions in beam delivery, not to mention potential damage to system components by 800 kW of beam power.

The CEBAF accelerator is composed of two parallel linear accelerators, connected head-to-tail by five 180-degree recirculation arcs at one end and four such arcs at the other. Beam from the injector enters the North Linac (NL), merging with the recirculated beam. The beams of differing energy are separated at the first "spreader" and transported to the "recombiner" at the entrance of the South Linac (SL). After acceleration, the beams are separated again at the second spreader region, where each beam is directed either into a recirculation arc for the next pass through the system or toward the end stations for experimental use.

During early operation of the CEBAF injector, we observed beam motion in the 45 MeV region on the scale of several millimeters [1]. The injector has been cleaned up well by means including the correction of grounding errors and the re-routing of some power distribution lines, but in commissioning the accelerator we are finding line-synchronous energy variation and millimeter scale steering perturbations in the main accelerator.

\*Work supported by U.S. D.O.E. contract #DE-AC05-84ER40150

## II. DATA ACQUISITION

The beam position monitor (BPM) system at CEBAF has a global trigger for synchronization with pulsed beam operation. We have provided a line-synchronous mode for the master system trigger, along with a programmable delay with respect to the AC line zero crossing. This delay allows the use of the beam position monitors (which have a 1 Hz update rate through the control system) as a multichannel data acquisition system, effectively a digital sampling oscilloscope, gathering synchronized orbit data throughout the accelerator as a function of phase delay with respect to the AC line. Measurement of the beam position in dispersive regions provides relative beam energy information at a resolution of approximately 0.001%[2].

The present injector line synchronous trigger uses a simple zero crossing detector, and has a jitter window of approximately 20 microseconds with respect to a line-synchronized phase locked loop. The programmable delay (16 bits with 1 microsecond resolution) spans the full 17 millisecond 60 Hz cycle. BPM data are logged for each of a series of values for the time delay with respect to the AC line trigger. For the measurements reported here, we used a 500 microsecond delay increment, cycling multiple times through the 60 Hz period.

The present BPM system has an analog bandwidth of approximately 50 kHz, so the measurements described here are not limited by the BPM hardware. Each position reading update to the control system consists of the average value from twelve sequential beam pulses, sampled approximately 65 microseconds into each macropulse (typically 100 microseconds in duration). The BPM hardware monitoring the various recirculated passes of the beam around the machine is multiplexed to the digitizers so that in each 1-second interval, each of the 5 passes is sampled 12 times. The precision of each averaged measurement at the 15 microampere beam current used for much of the recent commissioning operations is typically 0.2 millimeter. The averaging process strongly suppresses detection of perturbations at various harmonics of 5 Hz, but the harmonics of 60 Hz are unaffected.

## III. DATA ANALYSIS

The time structure of the position perturbations is well represented by the first three harmonics of the line frequency, dominated by the fundamental and third harmonic (see Figure 1). Ground loop current measurements made without the averaging limitations of the our BPM protocol are similarly dominated by the first and third harmonics of 60 Hz, supporting the idea that harmonics of the 60 Hz are most important. We have Fourier analyzed the position data for the sine and cosine com-

# MASTER

DISTRIBUTION OF THIS DOCUMENT IS UNLIMITED

This report has been reproduced from the best available copy.

Available to DOE and DOE contractors from the Office of Scientific and Technical Information, P.O. Box 62, Oak Ridge, TN 37831; prices available from (615)576-8401, FTS 626-8401.

Available to the public from the National Technical Information Service, U.S. Department of Commerce, 5285 Port Royal Rd., Springfield, VA 22161.

Price: Printed Copy A02  
Microfiche A01

**DISCLAIMER**

**Portions of this document may be illegible  
in electronic image products. Images are  
produced from the best available original  
document.**

ponents of the first three line harmonics. These Fourier amplitudes vary around the accelerator in the same way as the actual positions and angles, i.e., through propagation by the static transport properties of the magnetic lattice.

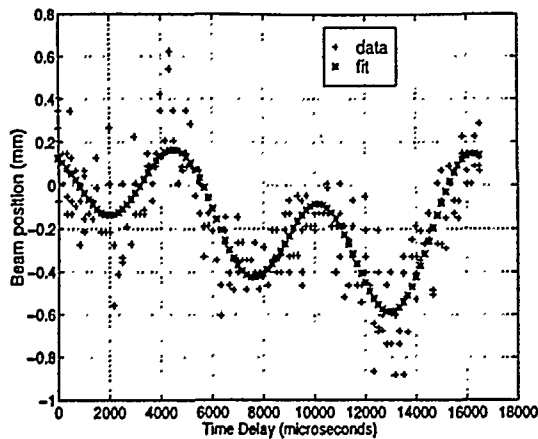


Figure 1: Example data showing the beam position dependence upon delay time. First and third harmonics are prominent. The BPM from which these data are taken is two-thirds of the way around the third recirculation arc. The "fit" curve uses the first three harmonics of 60 Hz.

We have used the RESOLVE [3] optics package to compare the static transport properties against the variations in beam position as a function of line trigger delay time. Along portions of the system with low levels of AC interference, the time dependence can be fit by time-dependence of the injection conditions. Distributed AC effects manifest themselves in a generally poor global fit of the beam position measurements using the static optics, although small segments of the machine may fit reasonably well. Significant point sources show up in the usual way as deviations between regions which can be individually fit to the static optics.

#### A. Measurements to date

Example data for beam position vs. line trigger delay are shown in Figure 1, along with the fit to the first three harmonics of 60 Hz. We found that the beam had measurable 60 and 180 Hz perturbations in steering and energy as it entered the North Linac (see figure 2), approximately 0.5 millimeter full span. We expected the Meissner effect of the superconducting acceleration cavities to shield the beam from most environmental effects in the tunnel, but we were unsure about effects in the unshielded regions outside the cryostats.

As can be seen from the data in the North Linac region, the transverse motion of the beam damps with the 10-fold acceleration through the linac. The span of the line-synchronous motion of the beam for 30 meters downstream from the linac and before it enters the spreader is below the 0.1 millimeter level. The amplitude remains small up to the first spreader region (vertical bends and quadrupoles). Here, both vertical and horizontal steering perturbations become visible, propagating through the first recirculation arc into the South Linac. The amplitude of the oscillation damps slightly through the South

Linac (where the energy increase is only a factor of two), growing again as the beam passes through the second spreader. The amplitude in the arcs is a factor of several higher than in the linacs, and essentially equal in Arcs 1 and 2.

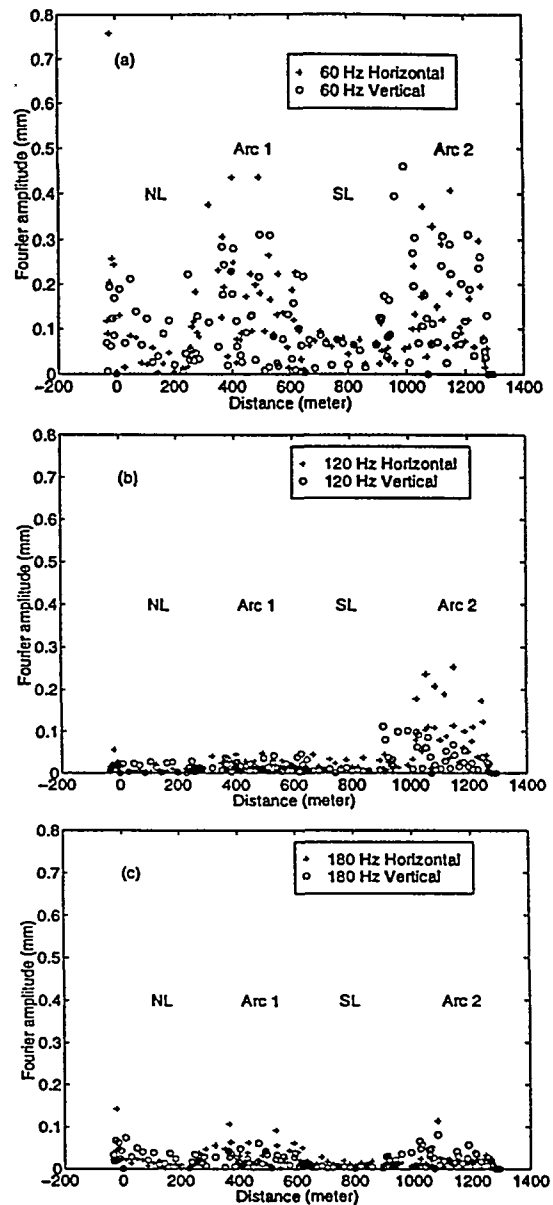


Figure 2: Fourier amplitudes of beam motion throughout 1st pass, combining the sine and cosine terms: (a) shows the 60 Hz component for single-pass beam through the linacs and the first two arcs; (b) shows the 120 Hz component; and (c) shows the 180 Hz component. The peak in horizontal amplitude in (a) near the entrance of the North Linac is in the dispersive region of the injection chicane, and is due to energy variation from the injector. The consistently larger amplitude of motion in the arcs is largely due to the bend dispersion.

In measurements taken with multiple-pass beam in the system, we can resolve meaningful data only in the regions where the beams of differing energy occupy separate beam-

lines until the multipass linac BPM system becomes operational. We find all beams carrying comparable steering perturbations in the separated regions, as might be expected from the above discussion. Comparison against static optics data for this configuration shows that the transport through the arcs is consistent with the static optics with time variations in both steering and energy, so the first three arcs appear to be relatively free of line-frequency sources. (Data in this set for the fourth and subsequent arcs is incomplete due to partial interception of beam at a septum upstream from the fourth arc.)

The propagation of the beam downstream from the vertical separation magnets of the spreaders to the point of injection into the arcs is also consistent with static optics, except for a localized perturbation coincident with the path length adjusting "dogleg" chicane magnets. These dogleg regions contribute horizontal (in the plane of the chicane) momentum kicks of similar magnitude to each beam, corresponding to a kick of approximately 5 microradian for the first pass (395 MeV in this instance) beam. This local perturbation was investigated, and a malfunction in the dogleg magnet supplies was found to be generating ripple of the proper magnitude to explain the effect. We have not yet identified a source for the horizontal and vertical perturbations observed at the spreader magnets.

In these and other measurements made to date, there is a clear increase in the 180 Hz component for the higher passes, becoming more significant than the 60 Hz component for the third and fourth passes.

Table 1: Sine and cosine components of energy variation for first, second, and third harmonics of 60 Hz, in parts per million. The arc 1 data represent the North Linac ripple alone, while the Arc 2 data represent the sum of North Linac and South Linac ripple. A weighted sum of these for comparison against the Arc 3 measurements is shown in the bottom row (see text). Discrepancies are typically 10 to 20 parts per million.

Harmonic Amplitudes of Energy Variations						
	60 Hz		120 Hz		180 Hz	
	sin	cos	sin	cos	sin	cos
Arc 1	-10	-66	+29	+12	+27	+3
Arc 2	-47	+27	+24	-2	+6	-19
Arc 3	-29	+17	+16	-13	+7	-18
Arc 1 + Arc 2	-35	-5	+27	+3	+14	-12

## B. Energy perturbations

The same analysis also provides a measure of line-synchronous energy variations, as the arcs include regions of dispersion up to approximately 2.5 meter. The energy variation for the first three line harmonics is shown in Table 1. The data of the table have precision of 10 parts per million (estimated from the observed scatter of 50 parts per million in energy estimates made from the same BPMs in real time, coupled with averaging over 25 times as many samples as are used in the on-line routine, and (2) from the residual errors of the fit to the data). The row labeled "Arc 1 + Arc 2" contains a weighted sum of the Arc 1 (North Linac ripple) and Arc 2 (North Linac plus South Linac ripple). For this run, the beam energies were 395 MeV in Arc 1, 750 MeV in Arc 2, and 1105 MeV in Arc 3. The injector energy lock was active for this run, compensating for the injector energy ripple. Therefore the absolute energy ripple in Arc 3 should be equal to the sum of the energy ripple in Arc 2 plus the contribution from the second pass through the North Linac. The discrepancies between the measured Arc 3 ripple and the weighted sums for Arcs 1 and 2 are typically in the 10 to 20 parts per million range, in reasonable agreement with the error estimates we have for the ripple determinations.

## IV. CONCLUSIONS

We have devised a method of taking beam position data throughout the CEBAF accelerator, using the BPM system in a sampling mode, to determine the line-synchronous beam position perturbation. We have found that comparison of these data against the measured static optics provides a useful means of identifying sources of line-frequency interference. We have identified microradian-level point sources of interference (magnet ripple) and have resolved relative energy variations of the beam at the 0.001% level. We anticipate that the techniques we are using will be useful for periodic measurement and long-term feedback correction of residual line-frequency variations at CEBAF.

## V. REFERENCES

- [1] R. Legg, et al., *Location and Correction of 60 Hz in the CEBAF injector*, this conference
- [2] J. van Zeijts, et al., *Slow Orbit and Energy Lock Systems at CEBAF*, this conference
- [3] B. Yunn, et al., *RESOLVE at CEBAF*, this conference

## DISCLAIMER

This report was prepared as an account of work sponsored by an agency of the United States Government. Neither the United States Government nor any agency thereof, nor any of their employees, makes any warranty, express or implied, or assumes any legal liability or responsibility for the accuracy, completeness, or usefulness of any information, apparatus, product, or process disclosed, or represents that its use would not infringe privately owned rights. Reference herein to any specific commercial product, process, or service by trade name, trademark, manufacturer, or otherwise does not necessarily constitute or imply its endorsement, recommendation, or favoring by the United States Government or any agency thereof. The views and opinions of authors expressed herein do not necessarily state or reflect those of the United States Government or any agency thereof.